I J C T A, 10(9), 2017, pp. 241-254 ISSN: 0974-5572

Preparation and Characterization of Nanostructured $Zn_{(X)}Fe_{(1-X)2}O_4$ (X=0.1 to 0.9)

A. Akshaykranth*, R. Karthik* and K. Venkateswara Rao, C.H. Shilpa Chakra****

ABSTRACT

This paperdescribes the preparation of Zinc Ferrite ($Zn_{(x)}Fe_{(1-x)2}O_4$ (X = 0.1, 0.2, 0.3, 0.4, 0.5, 0.6, 0.7, 0.8 and 0.9)) nanoparticlesusing low temperature combustion method. Also,investigates on the properties of $Zn_{(x)}Fe_{(1-x)2}O_4$ (X = 0.1, 0.2, 0.3, 0.4, 0.5, 0.6, 0.7, 0.8 and 0.9) nanoparticles with gradually increasing the concentration of Zinc percentage parallelly decreasing the iron percentage. The obtained powders are characterized by XRD, SEM, FTIR, TG-DTA and UV-visible spectroscopy. Thermal analysis has been done by thermo gravimetric-differential thermal analysis (TG-DTA), UV-visible data shows the optical characteristics of obtained $Zn_{(x)}Fe_{(1-x)2}O_4$.

Keywords: Zinc ferrite; XRD; SEM; FTIR; TG-DTA;

1. INTRODUCTION

Among the ferrite materials, zinc ferrite has many applications in various fields of industry like magnetic materials, gas sensor and absorbent material for hot-gas desulphurization [1]. Recently, it was found that Zinc ferrite is a promising semiconductor photo-catalyst for various processes due to its ability to absorb visible light, high efficiency, low cost and excellent photochemical stability. In addition, zinc ferrite shows potentially wide applications in photo induced electron transfer, photo-electrochemical cells and photo-chemical hydrogen production. Zinc ferrite can be synthesized by numerous methods, such as ceramic method, sol–gel, co-precipitation, ball-milling technique, hydrothermal synthesis and thermal decomposition[2].

The traditional bulk $ZnFe_2O_4$ is a normal spinel with Zn^{2+} ions only on the tetrahedral (A) sites and Fe^{3+} ions only on the octahedral (B) sites. It has antiferromagnetic properties below the Néel temperature of about 10 K and behaves paramagnetic at room temperature. Recent investigations of Nano-crystalline $ZnFe_2O_4$ have suggested that the cation distribution in this material is partly inverted and exhibits anomaly in its magnetization. The Néel temperature or magnetic ordering temperature (T_N), means that the temperature above which an antiferromagnetic material becomes paramagnetic. In which the thermal energy becomes large enough to destroy the microscopic magnetic ordering within the material [3-4]. Néel suggested that small antiferromagnetic particles can exhibit super-para magnetism and weak ferromagnetism due to uncompensated spins in the two sub lattices. One of the most challenging open questions in the study of spinel ferrite nanoparticles is the cation distribution between the two interstitial sites of the structure and its influence on the different properties of the ferrite materials. Indeed, the cation distribution over the tetrahedral and octahedral sites in the spinel-type lattice is strongly dependent on the ionic radii, concentration of the substituted divalent metal ions and the synthesis pathway. Large cation redistributions/inversion parameters can be obtained only by placing $ZnFe_2O_4$ into a non-equilibrium state [5-9].

* Dept. of Electronics & Communication Engineering MLR Institute of Technology Hyderabad, India, *Emails: akshaykranth417@gmail.com, karthik.r@mlrinstitutions.ac.in*

** Centre for Nanoscience & Technology IST – JNTU Hyderabad Hyderabad, India.

2. MATERIAL PREPARATION

One of the most widely used method for preparation of Zinc ferrite nano particles is the combustion synthesis route using a fuel. The fuels used may be glycine, citric acid or urea. The precursor material used for the synthesis of ZFO by solution combustion route are Zn $(NO_3)_2$ and Fe $(NO_3)_3$ solutions with a certain concentration level. The precursor materials are zinc nitrate ($Zn(NO_3)_2$), iron nitrate, (Fe $(NO_3)_2$) and glycine with high purity. Glycine has high heat combustion property. Hence it is generally used as organic fuel, providing a good platform for redox reactions during the course of combustion.

Figure 1: The Series of $Zn_{(x)}Fe_{(1-x)2}O_4$ (x=0.1, 0.2, 0.3,0.4, 0.5, 0.6, 0.7, 0.8 and 0.9) nanoparticle samples

Initially, zinc nitrate, iron nitrate and glycine are taken in the proper calculated ratio, and dissolved in a beaker while stirring slowly using a glass rod till a clear solution was obtained.

The prepared solution was evaporated on a hot plate in the temperature range up to 120°C resulting in the formation of a thick gel. The gel was kept on a hot plate for auto-combustion and was heated in the temperature range 180–200°C. The Nano crystalline $Zn_{(x)}$ $Fe_{(1-x)2}O_4$ (X = 0.1 to 0.9) Series was formed within a few minutes. It was sintered at 500°C, 600°C, 700°C and 800°C for about 4 h till it gives different coloured, shiny powder of Nano crystalline $Zn_{(x)}Fe_{(1-x)2}O_4$ (x = 0.1, 0.2, 0.3, 0.4, 0.5, 0.6, 0.7, 0.8 and 0.9) nanoparticles as shown in figure 1.

3. RESULTS AND DISCUSSIONS

3.1. X-Ray diffraction analysis (XRD) Analysis

X-ray diffraction pattern of the prepared nano size powder is shown in Figure 2.The structural properties, average crystallite size and phase identity of the Nano powders were determined by x-ray diffractometer. For this materials the *d* values are calculated using the Bragg's law. These calculated *d* values are compared with the *d* values of standard zinc ferrite JCPDS card no 89-1012.The average crystallite size of the powders is determined by the line-broadening method by using the Scherrer formula, as given below

$$D = \frac{K.\lambda}{\beta Cos\theta} \tag{1}$$

Where D is the average crystallite size in nm, λ (~ 0.154 nm) the wavelength of the X-rayRadiation, θ the Bragg's angle and B the full width at half maximum (FWHM) of the peak observed for the samples

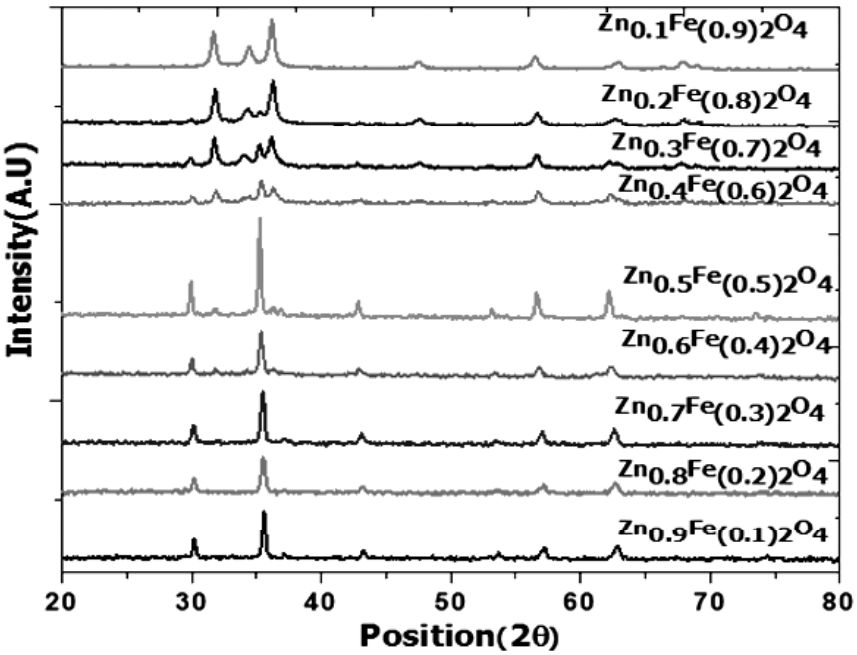

Figure 2: XRD pattern for $Zn_{(x)}Fe_{(1-x)2}O_4$ series

[10-11]. The series of $Zn_{(x)}Fe_{(1-x)2}O_4$(X = 0.1, 0.2, 0.3, 0.4, 0.5, 0.6, 0.7, 0.8 and 0.9) results were matched with JCPDS card number 89-1012. it has been matched exactly with the peaks corresponding to the planes (2 2 0), (3 1 1), (4 0 0), (4 2 2), (5 1 1), (4 4 0) and (5 5 3) observed at 30°, 35°, 43°, 57° and 62° respectively. The lattice parameters were obtained a=b=c= 0.84 nm.

This indicates that $Zn_{(x)}Fe_{(1-x)2}O_4$(X = 0.1 to 0.9) nano particles are in the cubic structure. The average crystallite sizes were measured as 27 nm, 26 nm, 22 nm, 27 nm, 33 nm, 19 nm, 20 nm, 20 nm and 21 nm for the entire $Zn_{(x)}Fe_{(1-x)2}O_4$(X = 0.1, 0.2, 0.3, 0.4, 0.5, 0.6, 0.7, 0.8 and 0.9)series.

The average crystalline size Verses oxidizers and Fuel weights were explained tentatively shown in fig 3. This can be depict that when $Fe(NO_3)_3$ weight is increasing the average crystalline size is also increasing.

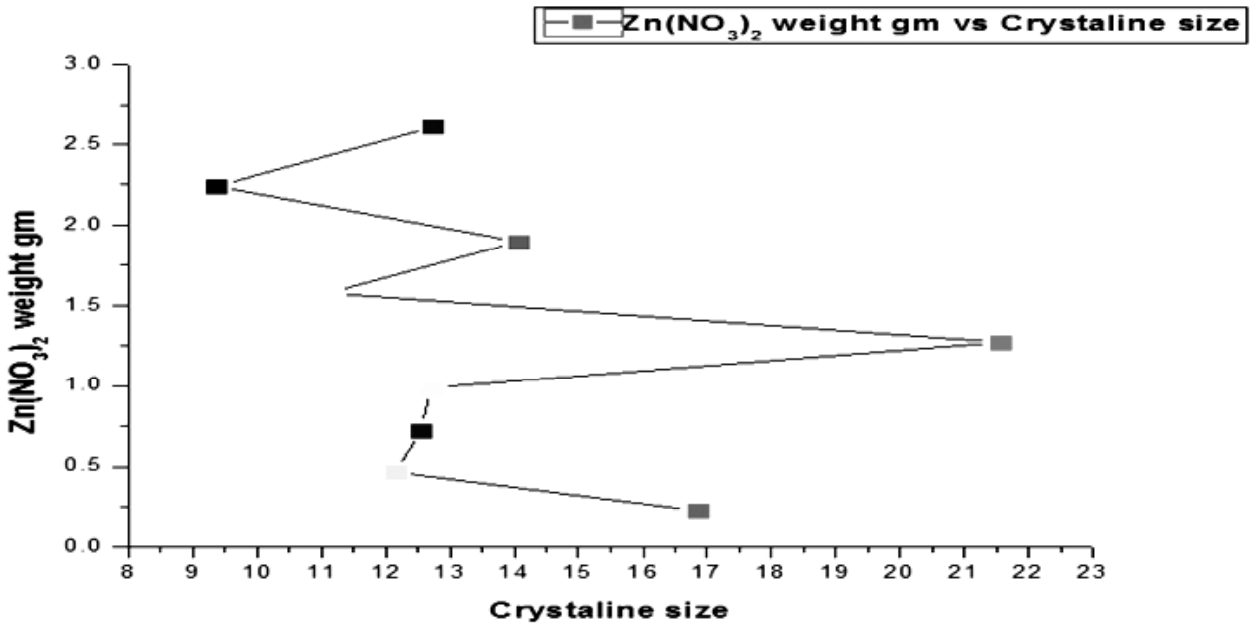

(a)

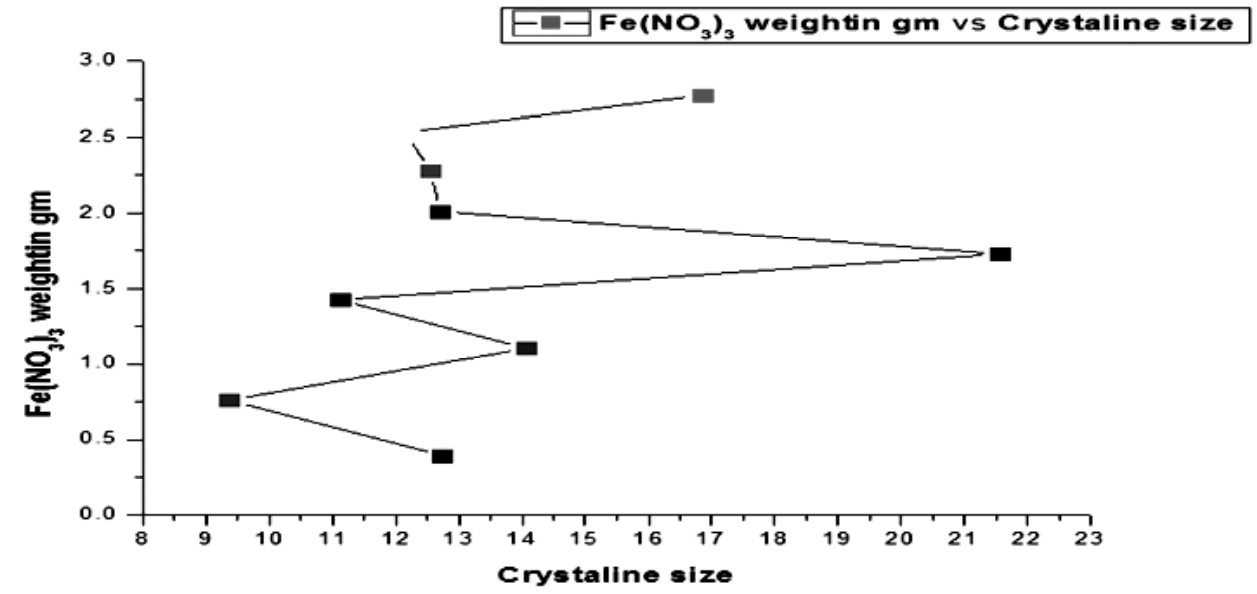

(b)

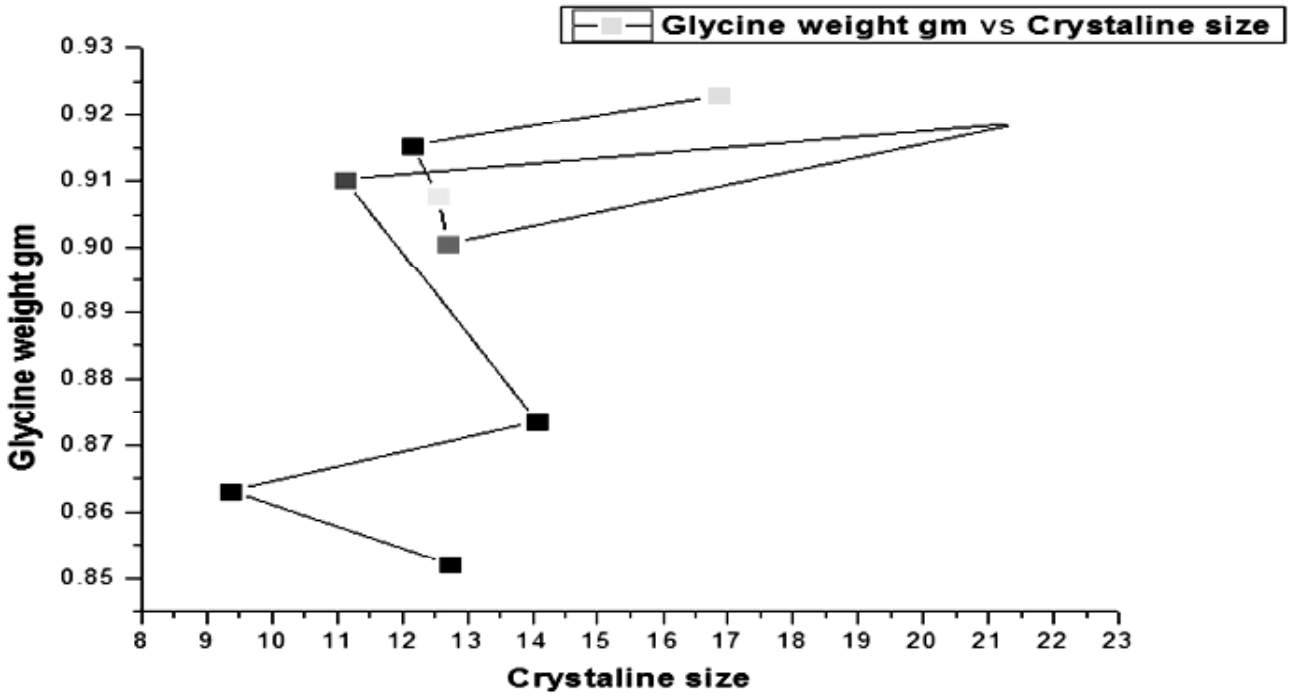

(c)

Figure 3: Shows (a) Average crystalline size verses $Zn(NO_3)_2$ weight, b)Average crystalline size verses $Fe(NO_3)_3$, b) Average crystalline size verses glycine

Where in the case of $Zn(NO_3)_2$, the weight of zinc nitrate is increasing the crystalline size is decreasing. No effect was observed in change of fuel weight.

3.2. Scanning Electron microscope (SEM) Analysis

The grain size, shape and surface properties like morphology were observed using Scanning Electron microscope analysis. The figure 4 represents the SEM picture of zincferrite series nanoparticles at 10ummagnification. The picture clearly reveals that the prepared sample is porous in nature.

SEM micrographs show remarkable change in the structure regarding porosity, grain size of sample illustrates in the Figure 4. From fig it can be concluded that has frothy and small holes within structure,

which may be due to escaping large number of gases during the combustion. It can be seen from the ûgure that sample exhibit network with voids and pores. The porosity in all cases is found to be entirely intergrannular. The formation of multigrain agglomerates observed in all samples consists of very ûne crystallites as they show strong tendency to form agglomerates.

These powders of $Zn_{(x)}Fe_{(1-x)2}O_4$ (x = 0.1, 0.2, 0.3, 0.4, 0.5, 0.6, 0.7, 0.8 and 0.9) show an increasing the porosity as expected due to the increasing the percentage of the Zinc while decreasing the percentage of ferrite. In the $Zn_{(0.5)}Fe_{(0.5)2}O_4$ (x = 0.5) sample porosity in between 2-200 nm was observed.

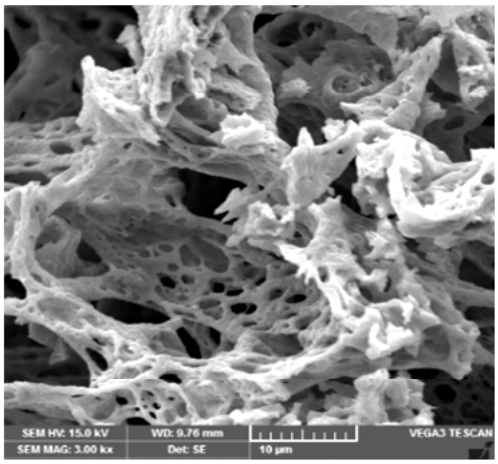

(a)

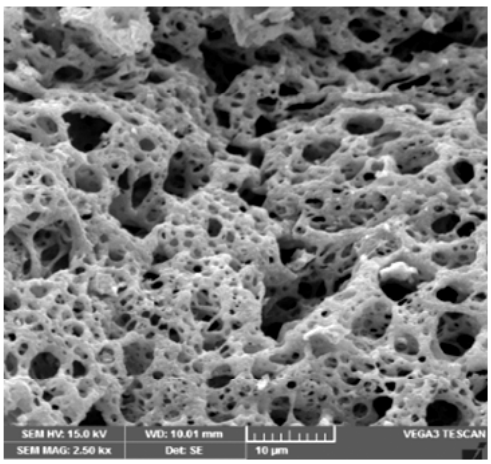

(b)

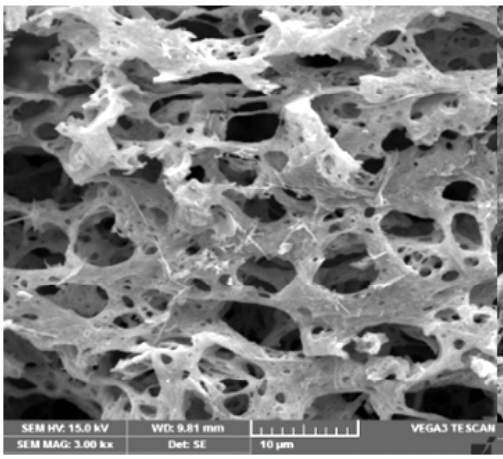

(c)

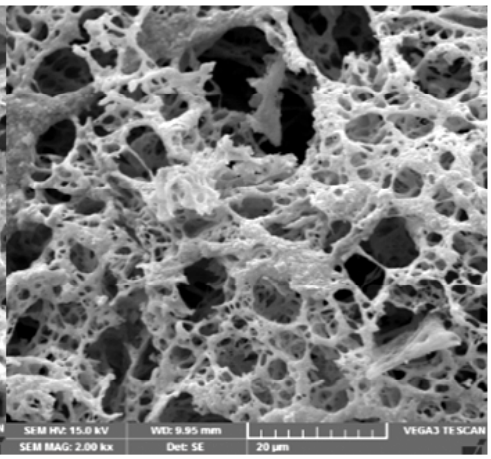

(d)

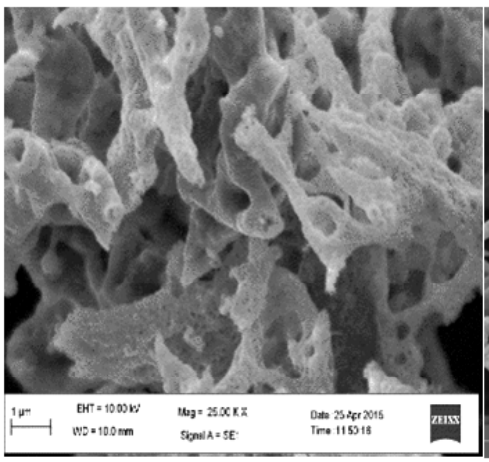

(e)

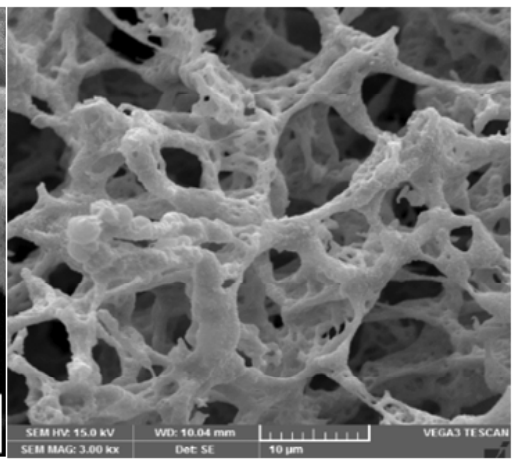

(f)

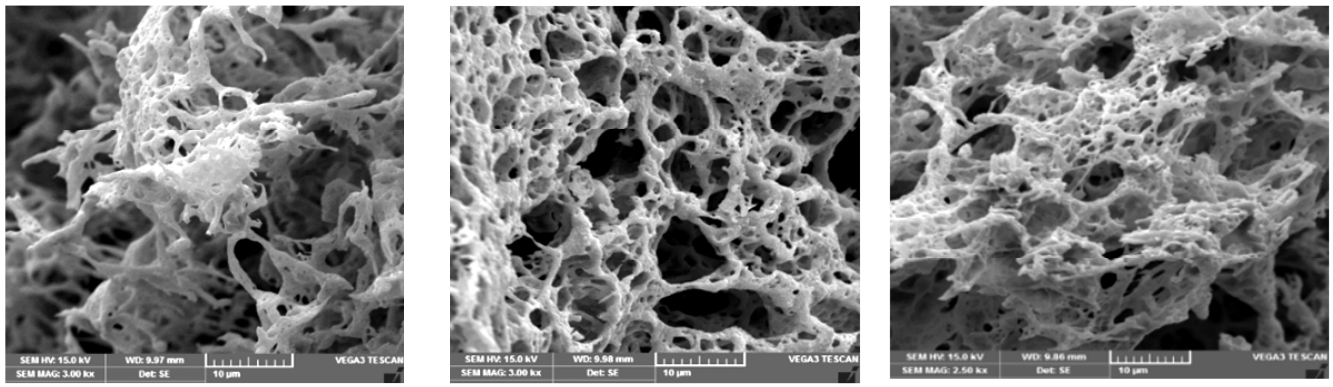

(g) **(h)** **(i)**

Figure 4: SEM Images of (a) $Zn_{0.1}Fe_{(0.9)2}O_4$, (b)$Zn_{0.2}Fe_{(0.8)2}O_4$ (c)$Zn_{0.3}Fe_{(0.7)}O_4$,(d)$Zn_{0.4}Fe_{(0.6)}O_4$, (e)$Zn_{0.5}Fe_{(0.5)2}O_4$, (f)$Zn_{0.6}Fe_{(0.4)2}O_4$, (g)$Zn_{0.7}Fe_{(0.3)2}O_4$,(h)$Zn_{0.8}Fe_{(0.2)2}O_4$, (i)$Zn_{0.9}Fe_{(0.1)2}O_4$

3.3. UV/Visible spectrometer Analysis

UV-visible absorption spectroscopy is widely being used technique to examine the optical properties of Nano sized particles. The Optical properties of the samples were studied using Systronics UV –Visible spectrometer 2202. From figure 5 the spectra exhibits between 200 and 1100 nm range.

Figure 5 depict the reflectance spectra of pure and Zinc ferrite nanoparticles in the spectral range of 200-300nm. It is a clear all the samples show optical properties in the visible region. In $Zn_{(x)}Fe_{(1-x)2}O_4$ (x = 0.5) sample reflectance percentage decreasing. Which has equal Zn-Fe percentage. But in the case of other samples $Zn_{(x)}Fe_{(1-x)2}O_4$ (x = 0.1, 0.2, 0.3, 0.4, 0.6, 0.7, 0.8 and 0.9) reflectance percentage almost equal. All the samples in the series represents two peaks around 240 nm and 250nm wavelength with small blue shift and red shift variation with respect to Nano size in the particles.

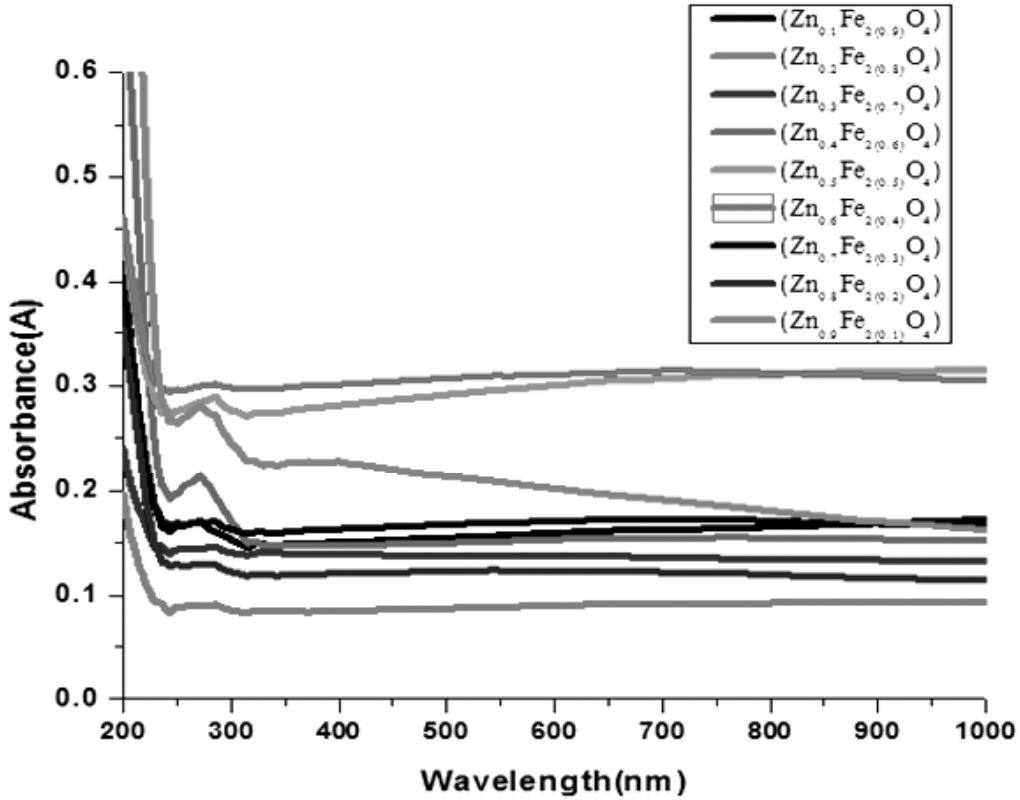

Figure 5: Reflectance spectra of $Zn_{(x)}Fe_{(1-x)2}O_4$ (x = 0.1, 0.2, 0.3, 0.4, 0.5, 0.6, 0.7, 0.8 and 0.9) nanoparticles

3.4. Thermo gravimetric/Differential thermal analysis (TG-DTA) Analysis

TG & DTA curves of $ZnFe_2O_4$series nanoparticles are as shown in Figure 6. The temperature range is 0°C to 800°C. In TG analysis, the thermal properties were attained for the samples using TG-DTA.

The percentage weight loss is calculated from TG graph using the formula.

$$\%\ weight\ loss = \frac{Initial\ weight\ (wi) - final\ weight\ (wf)}{Initial\ weight} * 100 \quad (2)$$

we can observe weight loss of the samples observed at room temperature to 100ºC due to the evaporation of water molecules, whereas 100ºC to 400ºC the weight loss caused by evaporation of inorganic materials. After 400ºC the weight loss occurs due to the evaporation of un-reacted materials which is involved in the samples. The total weight loss of the sample was measured $ZnFe_2O_4$ Nano particles as 1.4%, 12%, 10%, 10%, 12%, 10%, 12%, 12% and 2%. From these results 1.4% shows the $Zn_{0.1}Fe_{0.9}O_4$ shows the least weight loss in the series.

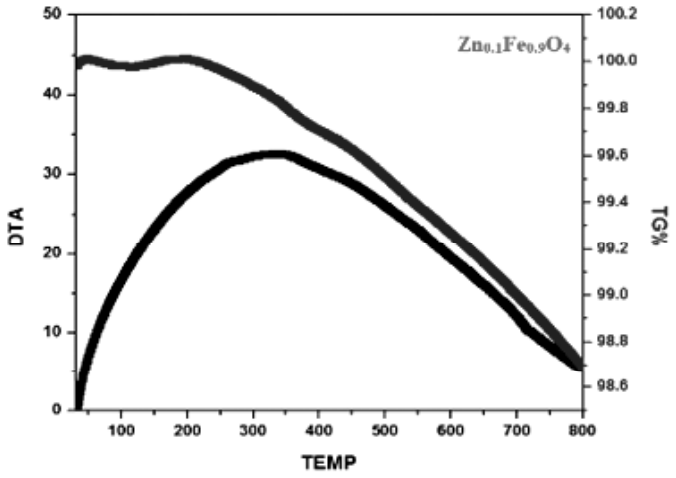

(a)

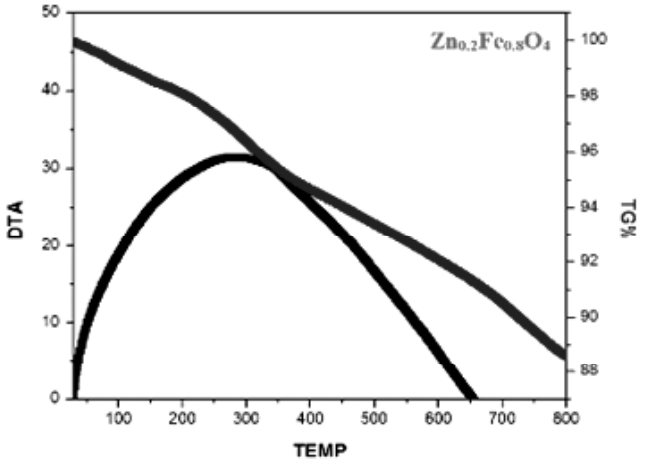

(b)

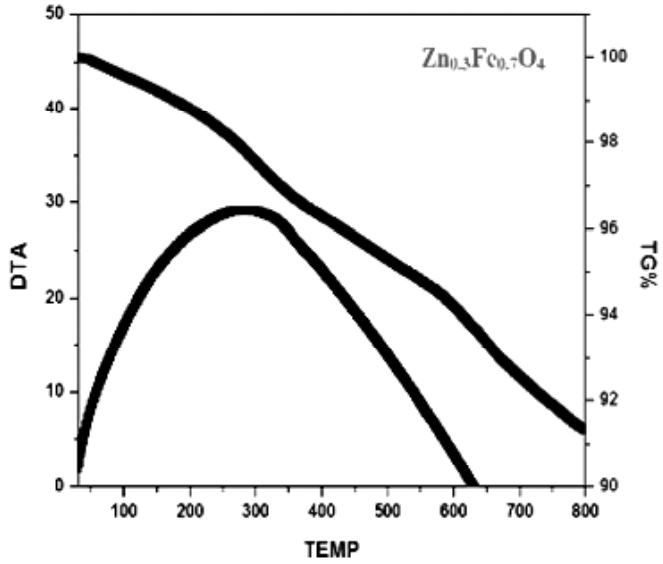

(c)

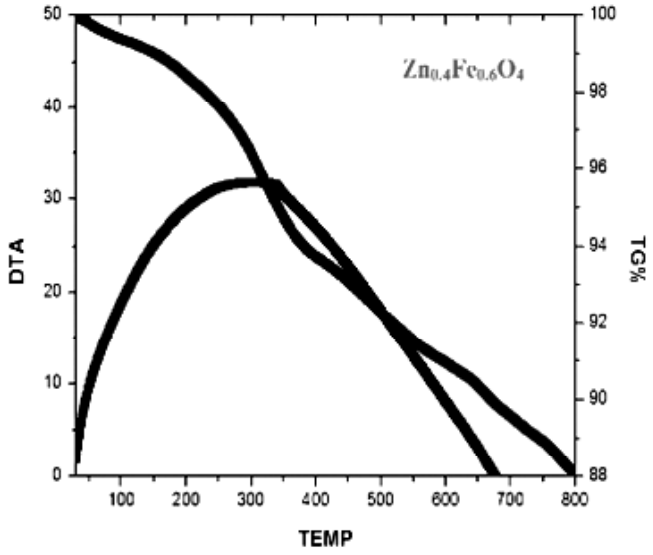

(d)

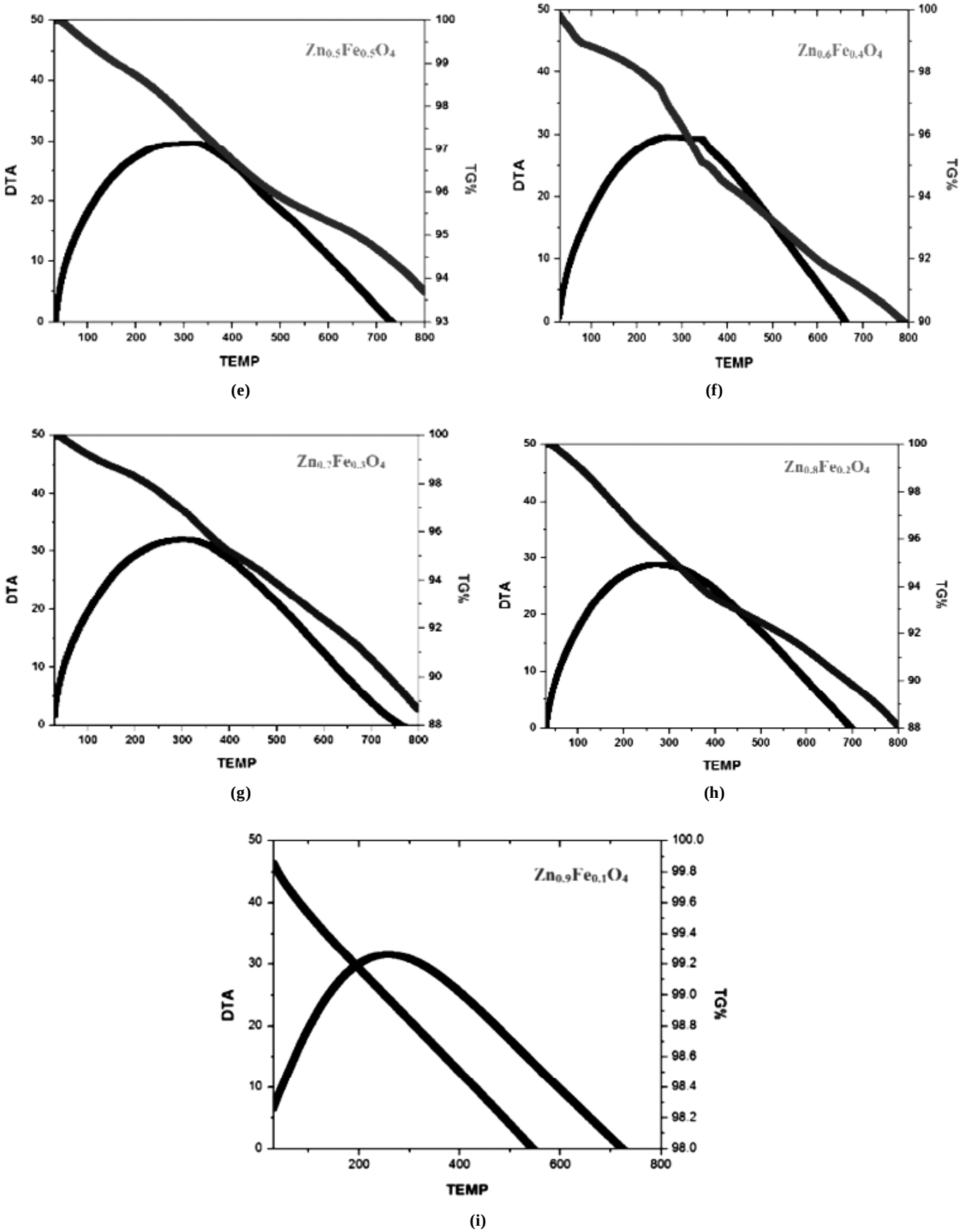

Figure 6: TG-DTA Curves of (a) $Zn_{0.1}Fe_{(0.9)2}O_4$, (b)$Zn_{0.2}Fe_{(0.8)2}O_4$ (c)$Zn_{0.3}Fe_{(0.7)}O_4$,(d)$Zn_{0.4}Fe_{(0.6)}O_4$, (e)$Zn_{0.5}Fe_{(0.5)2}O_4$, (f)$Zn_{0.6}Fe_{(0.4)2}O_4$, (g)$Zn_{0.7}Fe_{(0.3)2}O_4$, (h)$Zn_{0.8}Fe_{(0.2)2}O_4$, (i)$Zn_{0.9}Fe_{(0.1)2}O_4$

3.5. Fourier transform infrared spectroscopy (FTIR) Analysis

FTIR spectrometer is used to identify functional groups in a sample as they have their characteristic fundamental vibrations which gives rise to absorption at certain frequency range in the spectrum. The spectrum is commonly presented as transmittance versus wavenumber. Each band in a spectrum can be attributed to stretching or bending mode of a band. The figure 7 shows IR spectra of nanostructured zinc ferrite series. The analysis was done in the range of 500 cm^{-1} to 4000 cm^{-1}.

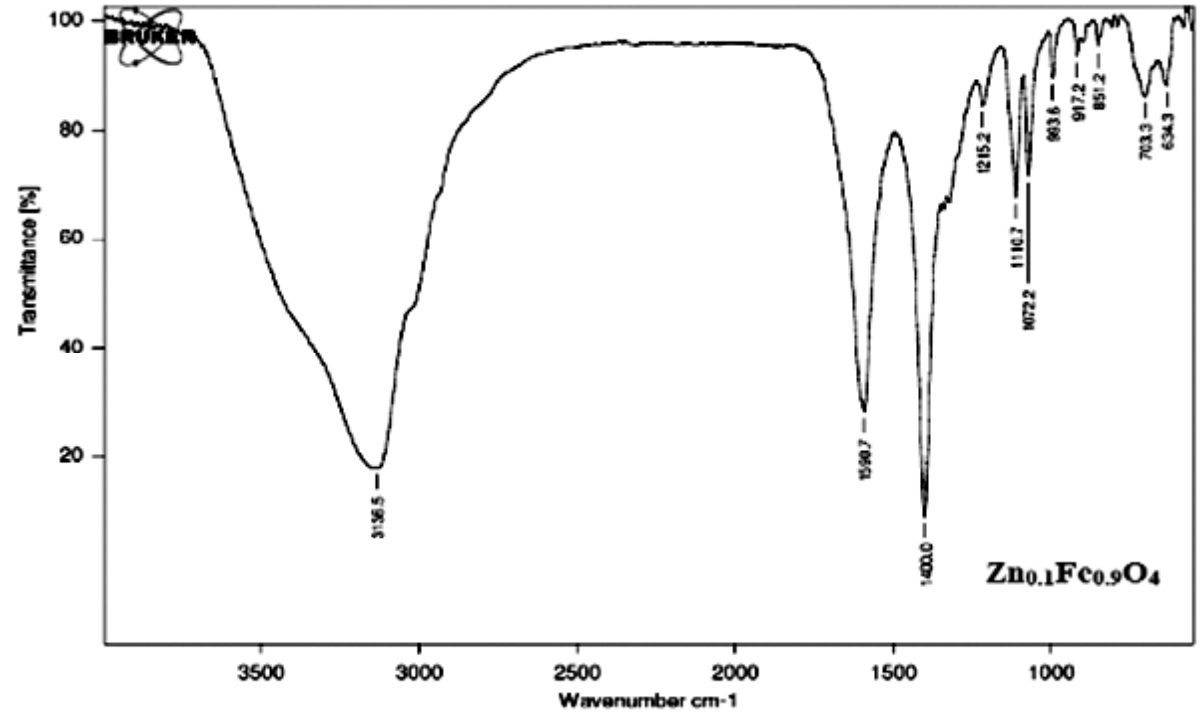

(a)

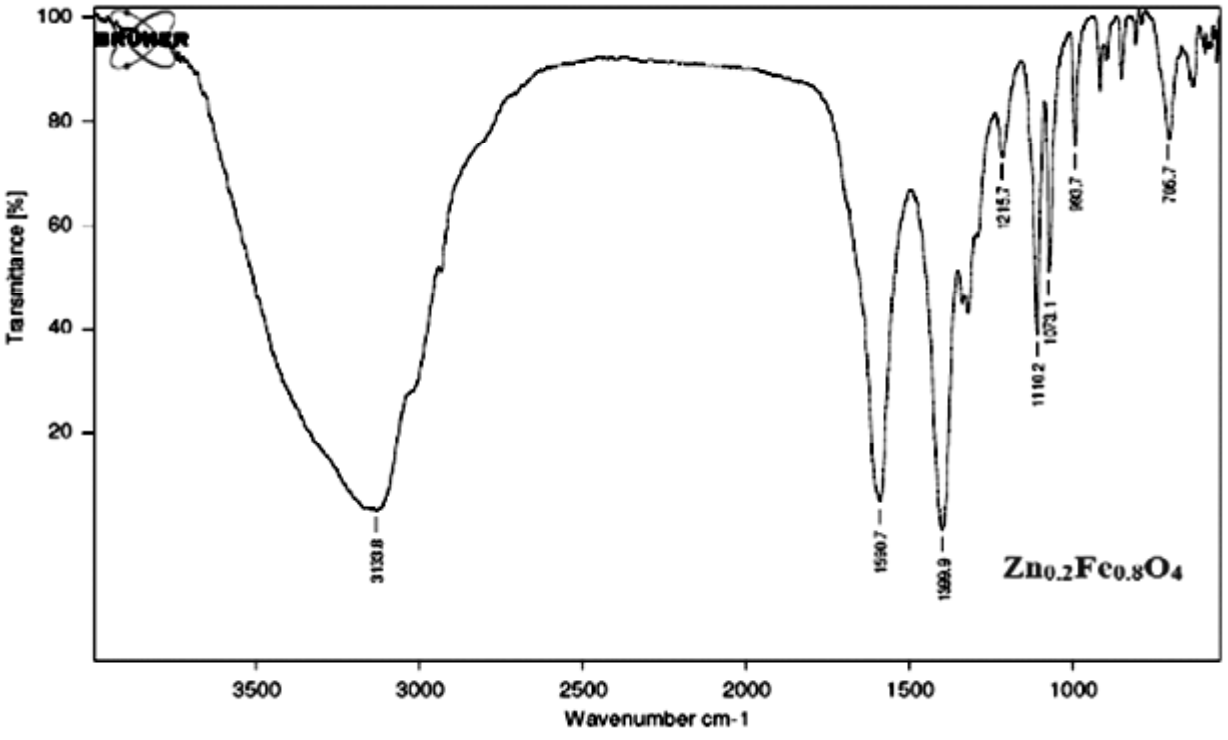

(b)

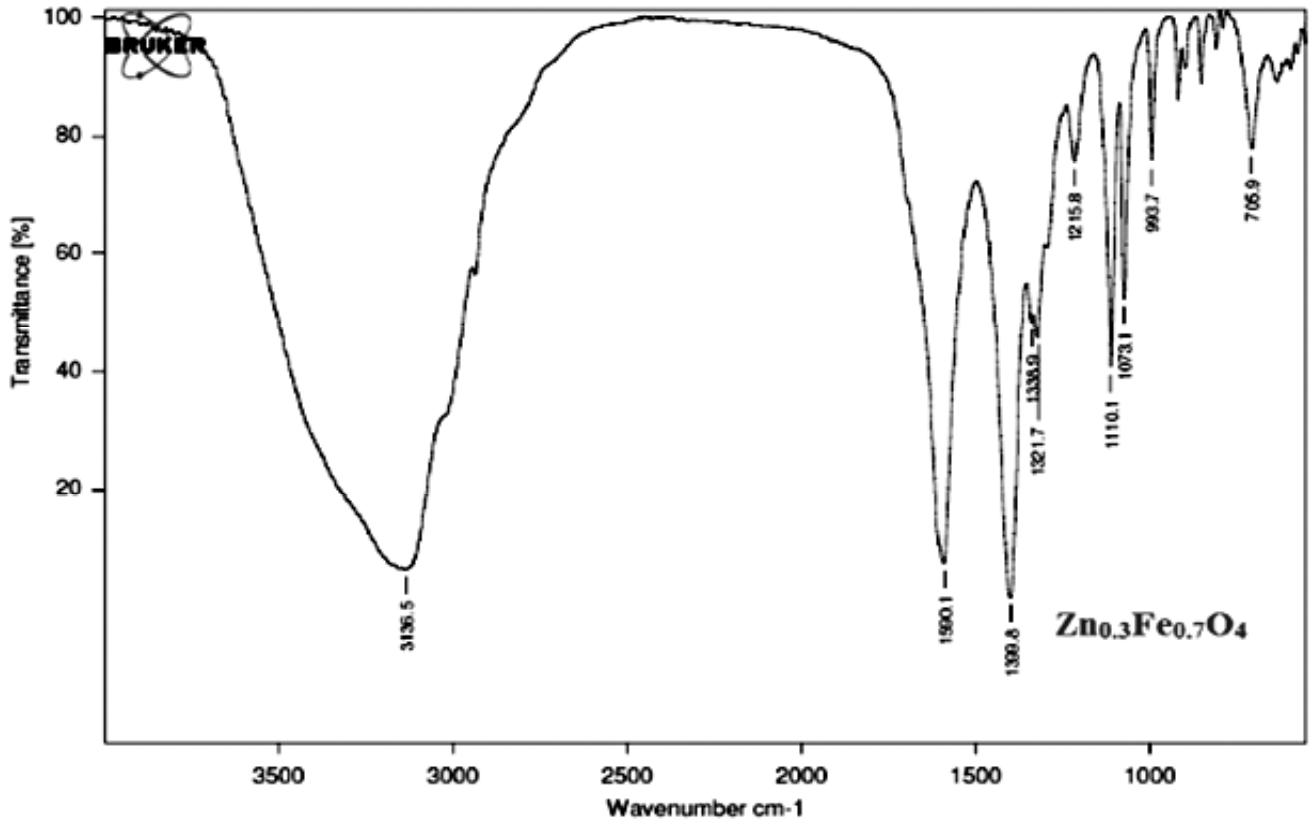
BRUKER
Transmittance [%]
100
80
60
40
20
3135.5
1590.1
1388.8
1321.7
1338.9
1215.8
1110.1
1073.1
993.7
765.9
Zn0.3Fe0.7O4
3500
3000
2500
2000
1500
1000
Wavenumber cm-1

(c)

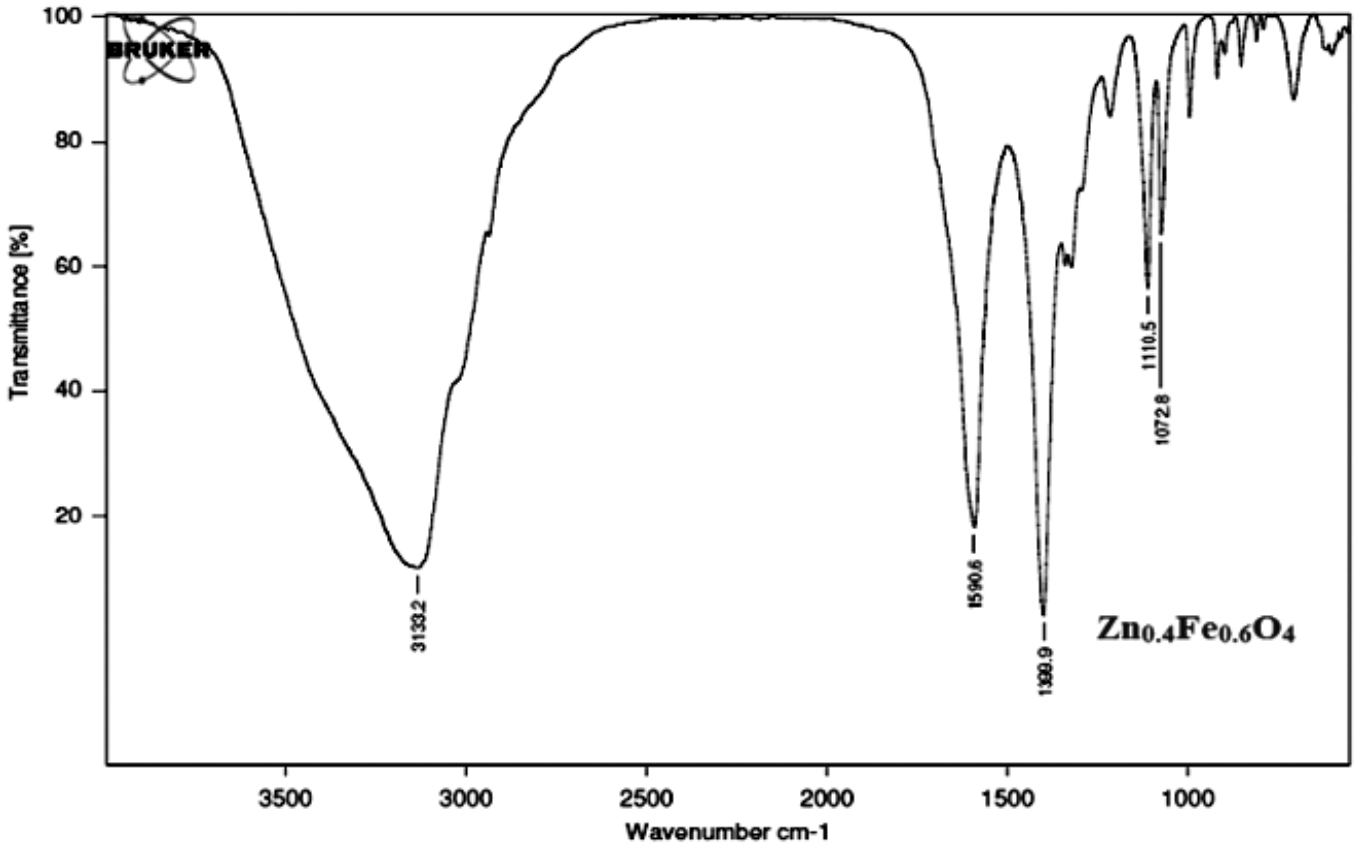
BRUKER
Transmittance [%]
100
80
60
40
20
3133.2
1590.6
1389.9
1110.5
1072.8
Zn0.4Fe0.6O4
3500
3000
2500
2000
1500
1000
Wavenumber cm-1

(d)

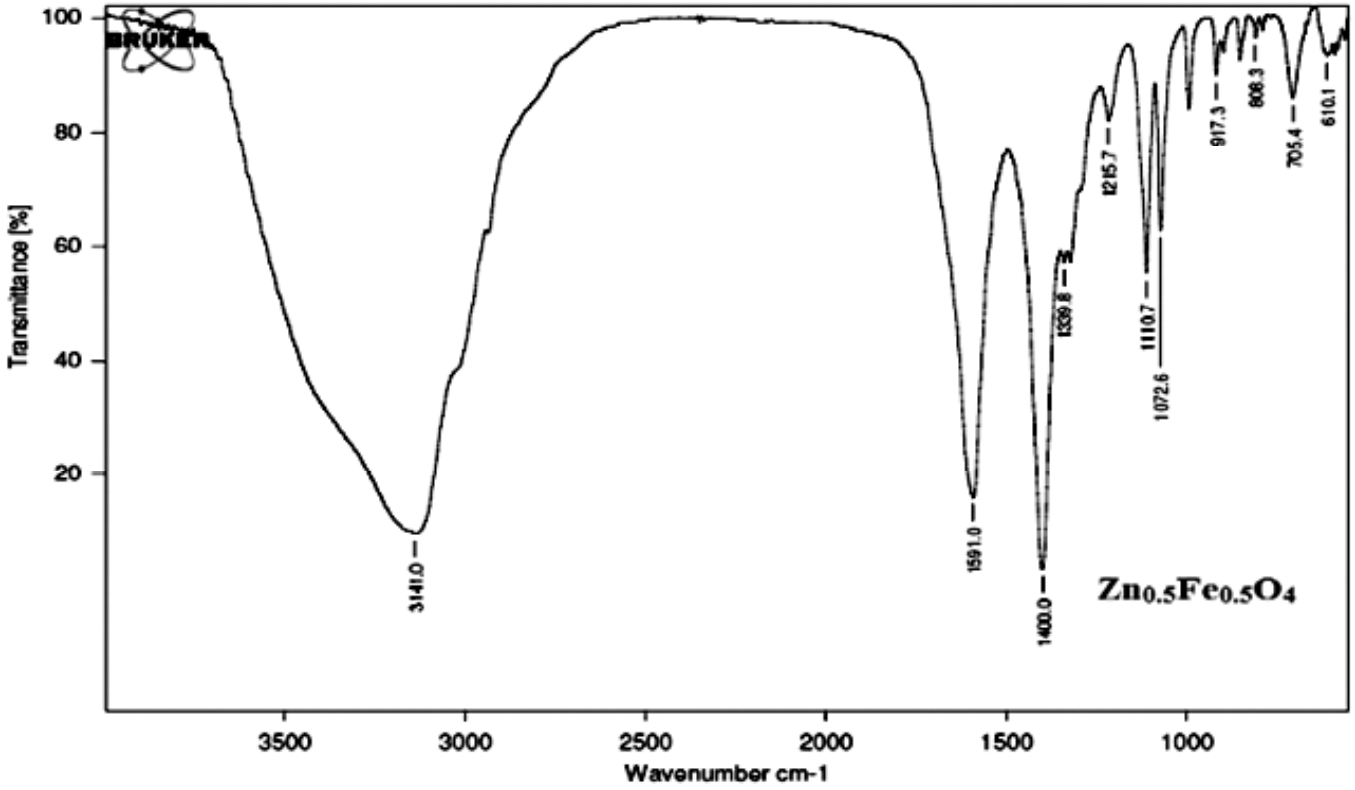
BRUKER
Transmittance [%]
100
80
60
40
20
3500
3000
2500
2000
1500
1000
Wavenumber cm-1
3141.0
1591.0
1400.0
1339.8
1215.7
1110.7
1072.6
917.3
806.3
705.4
610.1
Zn0.5Fe0.5O4

(e)

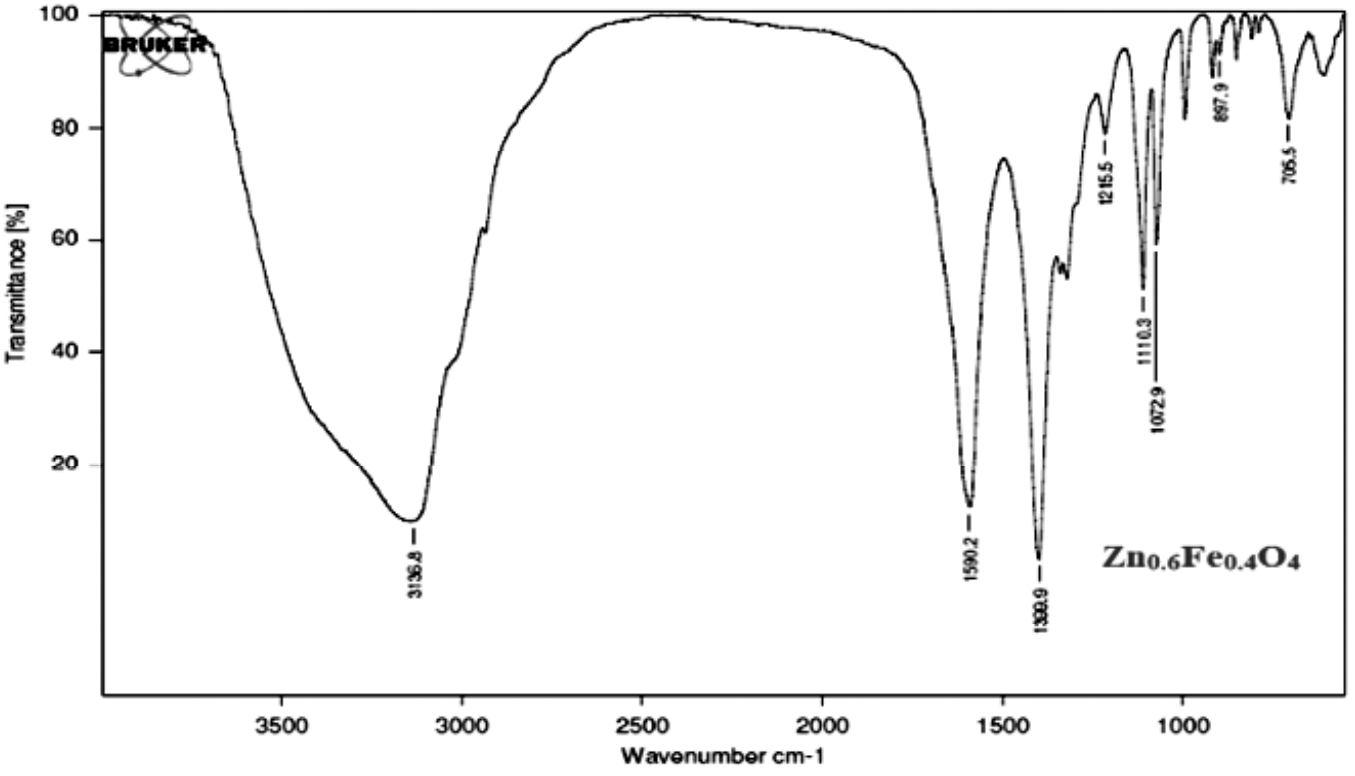
BRUKER
Transmittance [%]
100
80
60
40
20
3500
3000
2500
2000
1500
1000
Wavenumber cm-1
3136.8
1590.2
1399.9
1215.5
1110.3
1072.9
897.9
705.5
Zn0.6Fe0.4O4

(f)

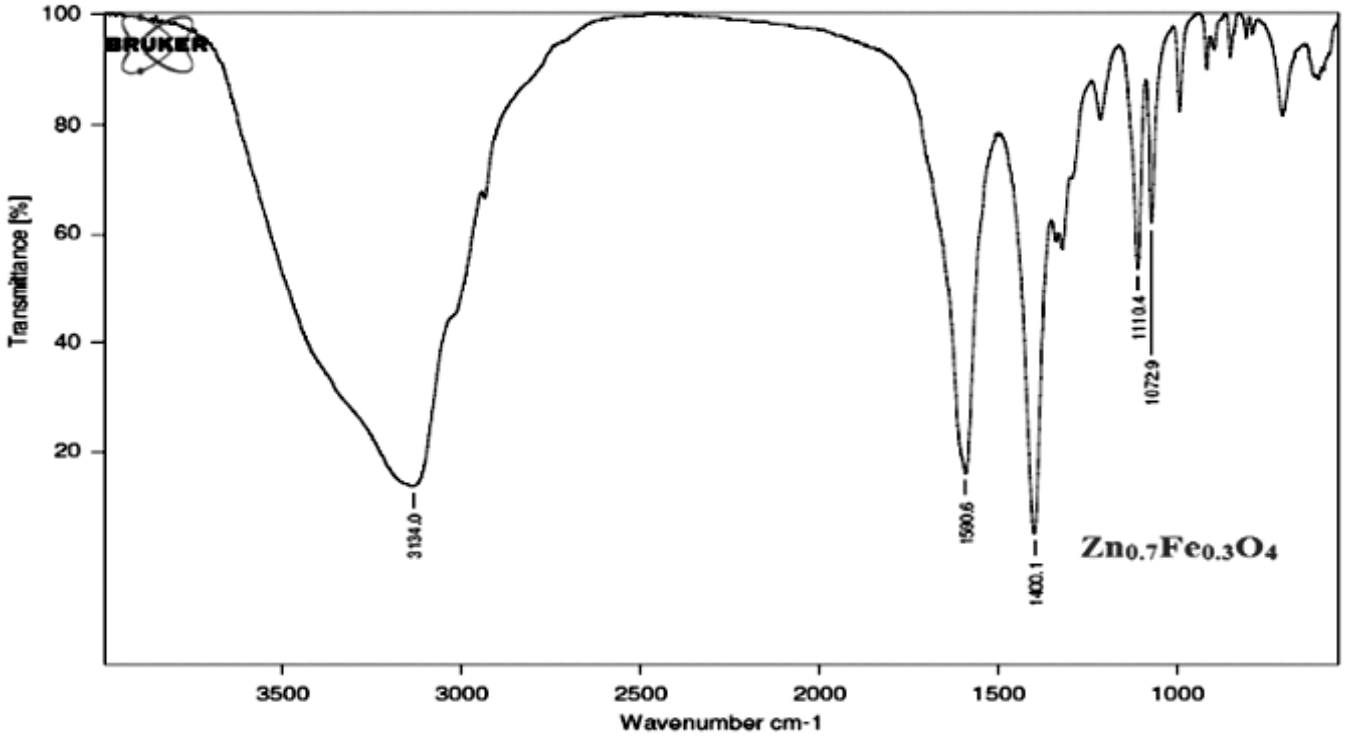

(g)

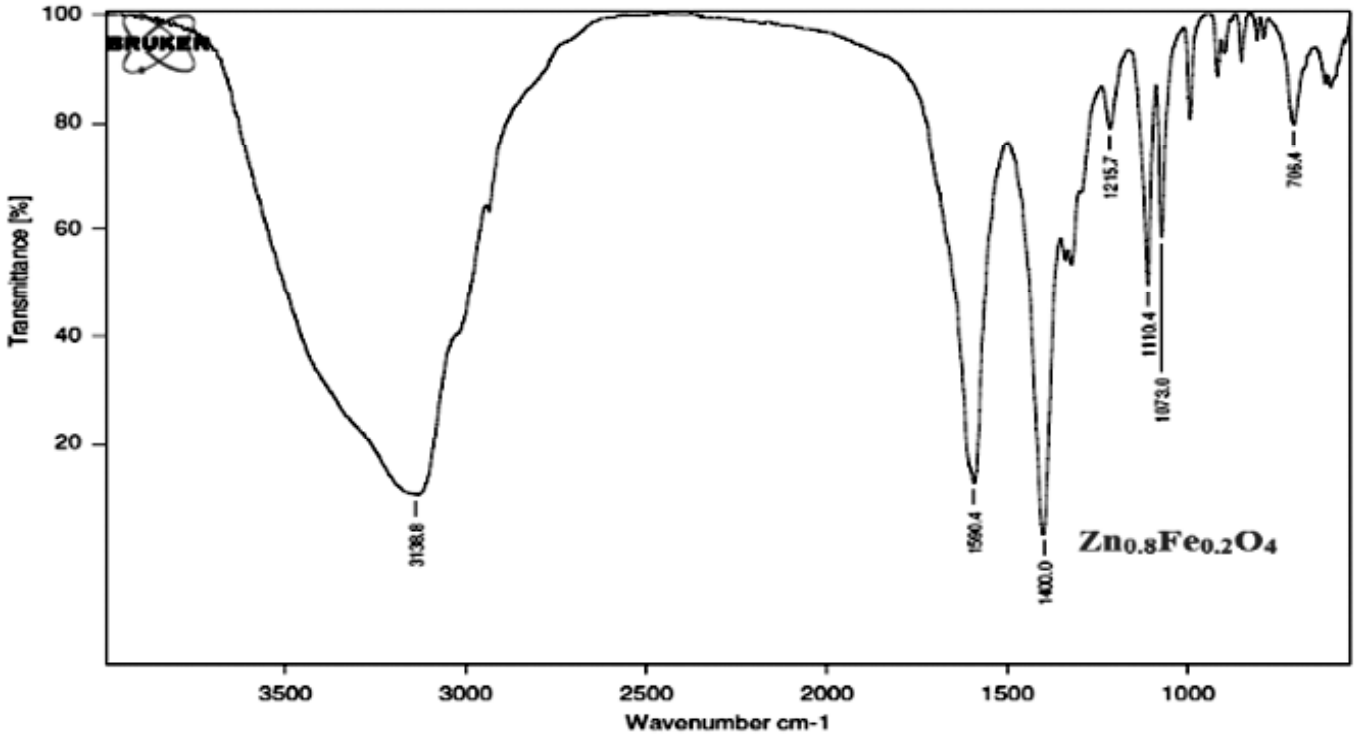

(h)

The absorption peaks at 3134-3141cm^{-1} meansintermolecular hydrogen bond (O–H) existing between the adsorbed water molecules and indicates the higher amount of hydroxyl group. The peaks at 1110–1072 cm^{-1} of C–O stretching and peaks at 1590-1400cm^{-1} may be produced due to symmetric stretching of CH_2 and CH_3 groups. The characteristic peaks at 705cm^{-1} become stronger, indicating the formation of stretching mode of $Zn_{(x)}Fe_{(1-x)2}O_4$ (x=0.1,0.2,0.3,0.4,0.5,0.6,0.7,0.8 and 0.9) nanoparticles.

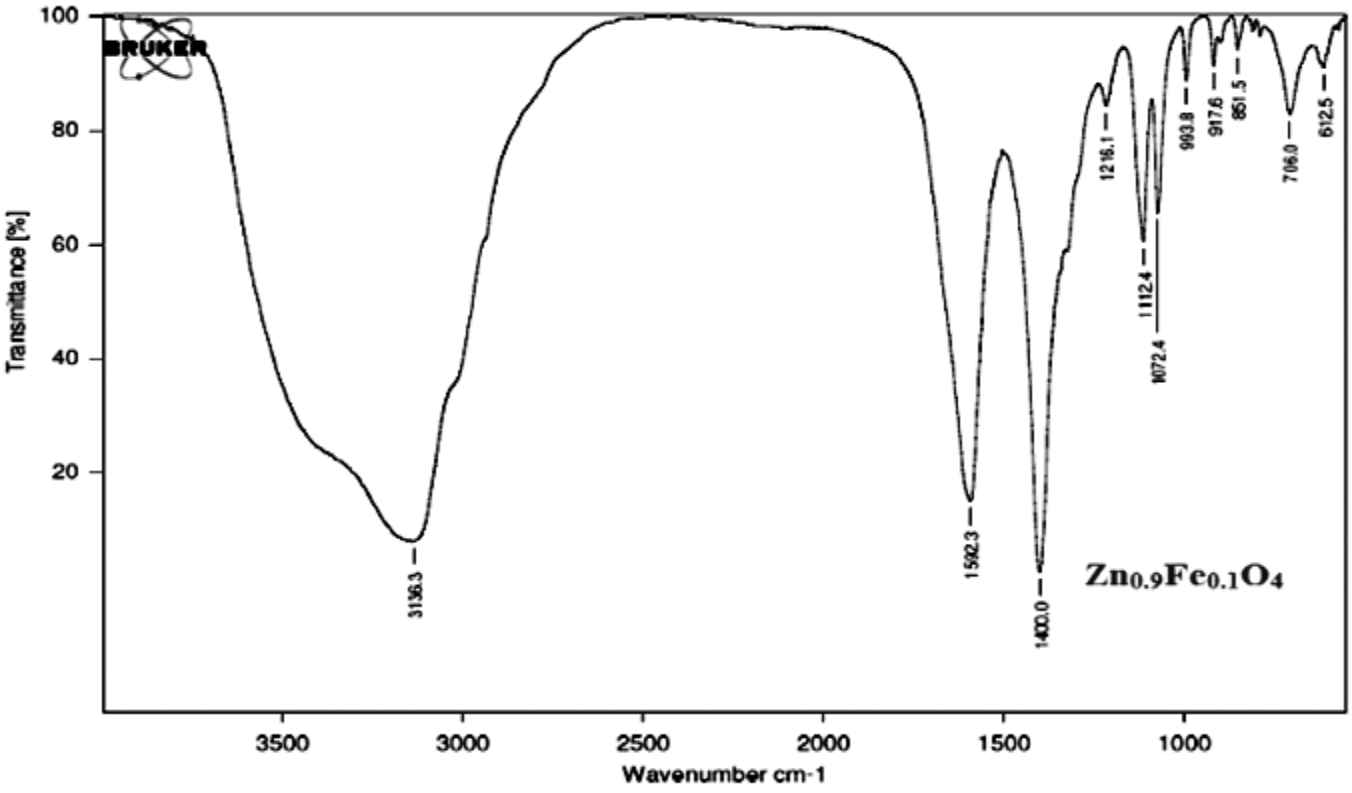

(i)

Figure 7: FTIR spectra for (a) $Zn_{0.1}Fe_{(0.9)2}O_4$, (b)$Zn_{0.2}Fe_{(0.8)2}O_4$ (c)$Zn_{0.3}Fe_{(0.7)}O_4$,(d)$Zn_{0.4}Fe_{(0.6)}O_4$, (e)$Zn_{0.5}Fe_{(0.5)2}O_4$, (f)$Zn_{0.6}Fe_{(0.4)2}O_4$, (g)$Zn_{0.7}Fe_{(0.3)2}O_4$, (h)$Zn_{0.8}Fe_{(0.2)2}O_4$, (i)$Zn_{0.9}Fe_{(0.1)2}O_4$

4. CONCLUSION

The series of $Zn_{(x)}Fe_{(1-x)\ 2}O_4$(X = 0.1, 0.2, 0.3, 0.4, 0.5, 0.6, 0.7, 0.8 and 0.9) Nano particles were successfully synthesized by low temperaturecombustion method. The structural properties studied using XRD reveals a good crystalline behavior and the average crystallite size. All the results from particle analyzer are in good agreement with the XRD results of crystallite sizes. The Surface morphology of the samples studied by using SEM showed agglomerated clusters resulting in more defects in the crystal so that the crystallinity of the powders was affected and the average particle size coincides with XRD data.From the UV-Vis studies it is clearly seen there is an increasesand decreases in absorbance on different concentration of zinc ferrite Nano particles. The FTIR analysis reveals that the bond structure of spinal structure and Zn-Fe-O has not been modified in Zinc Ferrite samples. Thermal analysis done by Thermo gravimetric Differential thermal analysis (TG/DTA) shows with the increase and decrease weight loss of the different concentration of the $Zn_{(x)}Fe_{(1-x)\ 2}O_4$(X=0.1, 0.2, 0.3, 0.4, 0.5, 0.6, 0.7, 0.8 and 0.9) Nano particles. The weight loss process becomes sharp and steady, indicating the formation of crystalline solid phases.

ACKNOWLEDGMENT

The authors express their deep sense of gratitude to Dr. K Venkateshwara Rao and Dr. CH Shilpa Chakra, Centre for Nano Science and Technology, IST, JNTU-Hyderabad for giving this opportunity to carry out the Synthesis, Fabrication and Characterization works at CNST department.

REFERENCES

[1] M. Mozaffari · H. Masoudi, “Zinc Ferrite Nanoparticles: New Preparation Method and Magnetic Properties”J Supercond Nov Magn, 27:2563–2567, 2014.

[2] N. M. Deraz, A. Alarifi “Microstructure and Magnetic Studies of Zinc Ferrite Nano-Particles” Int. J. Electrochem. Sci., 7,6501–6511, 2012.

[3] N. Ponpandian, A. Narayanasamy, C. N. Chinnasamy, “Néel temperature enhancement in nanostructured nickel zinc ferrite”Applied Physics Letters , Volume 86, April 2005.

[4] Hayoung Yoon, Ji Sung Lee, Ji Hyun Min, JunHua Wu, and Young Keun Kim, “Synthesis, microstructure, and magnetic properties of monosizedMn $_x$ Zn $_y$ Fe$_{3“x”y}$ O$_4$ ferrite nanocrystals”Nanoscale Res Lett. 2013.

[5] A. Kmita , A. Pribulova*et al* “USE OF SPECIFIC PROPERTIES OF ZINC FERRITE IN INNOVATIVE TECHNOLOGIES”Arch. Metall. Mater., Vol. 61, No 4, p. 2141–2146,2016.

[6] N. M. Deraz, and A. Alarifi “Synthesis and Physicochemical Properties of Nanomagnetic Zinc Ferrite System”,Int. J. Electrochem. Sci., 7,3798–3808, 2012.

[7] N.M. Deraz, A. Alarifi, “Synthesis and characterization of pure and Li_2O doped $ZnFe_2O_4$nanoparticles via glycine assisted route Polyhedron 28, 4122–4130, 2009.

[8] N. M. Deraz,A. Alarifi “Microstructure and Magnetic Studies of Zinc Ferrite Nano-Particles” Int. J. Electrochem. Sci., 7, 6501–6511, 2012.

[9] X. Chu, X. Liu, and G. Meng, “Preparation and gas sensitivity properties of $ZnFe_2O_4$ semiconductors,” Sens. Actuators B, vol. 55, no. 1, pp. 19–22, Apr. 1999.

[10] Rajinder Kumara , Ragini Raj Singha and P. B. Barmana “COBALT DOPED NICKEL ZINC FERRITE NANOPARTICLES – XRD ANALYSES AN INSIGHT”, International Journal of Scientific & Engineering Research, Volume 5, Issue 5, ISSN 2229-5518, May-2014 .

[11] IsrafUd Din, S. Tasleem, A. Naeem, Maizatul S. Shaharun, Ghassan M.J. Al Kaisy “Zinc Ferrite Nanoparticle Synthesis and Characterization; Effects of Annealing Temperature on the Size of nanoparticles”Australian Journal of Basic and Applied Sciences, 7(4): 154-162, ISSN 1991-8178.2013.